Structure of drawn fibres: 3. Neutron scattering studies of polyethylene fibres drawn beyond the neck

The late D. M. Sadler and P. J. Barham
H. H. Wills Physics Laboratory, University of Bristol, Tyndall Avenue, Bristol BS8 1TL, UK
(Received 30 January 1989; revised 20 April 1989; accepted 24 April 1989)

Results of neutron scattering experiments performed on polyethylene fibres drawn beyond the neck are reported. Data are reported for fibres with total draw ratios up to ~40 and tensile moduli up to ~100 GPa. It is shown that on post-neck drawing at temperatures below ~80°C the molecules deform affinely with the sample. At higher drawing temperatures the molecules deform to a lesser extent than the bulk material. It is further demonstrated that in all cases the final tensile modulus of the drawn fibres is a unique function of the *molecular* draw ratio.

(Keywords: drawing; fibre formation; high modulus fibres; neutron scattering; polyethylene)

INTRODUCTION

In the previous two papers of this series[1,2], we have addressed the issue of how molecules deform during necking. We have shown, for melt-crystallized material, that below ~60°C the molecules deform more or less affinely with the sample through the neck; and that at higher drawing temperatures, local melting occurs, which leads to isotopic segregation and obscures the neutron scattering signals from individual molecules[1]. For the case of solution-crystallized material the molecules are not initially arranged randomly, but are contained in 'superfolded sheets' within the chain-folded lamellar crystals[3]; these crystals lie with their c axes normal to the draw direction. After necking, we find that the molecules have rotated so that they now lie mainly parallel to the draw direction, but they have suffered little overall extension[2]. The purpose of the present paper is to address the question of how the molecules deform when fibres (which have been produced by drawing through a neck) are stretched to higher draw ratios.

The achievement of high draw ratios is a subject of importance in its own right; this is due to the fact that, as the draw ratio increases, so do the fibre modulus and strength. The work of Ward and his colleagues[4–6] in the 1970s showed that melt-crystallized polyethylene could be drawn to total draw ratios of up to 30, so that the resulting fibres had tensile moduli as high as 75 GPa. It was noted that the draw ratio attained depended on the polymer molecular weight (and its distribution), and, to a lesser extent, on the crystallization conditions[4]. Further, it was found that (for a particular drawing temperature) the modulus was a unique function of the draw ratio[6,7]. The most significant drawback of this approach was that the high draw ratios could only be achieved using comparatively low-molecular-weight polymers which, in turn, led to only moderate strengths.

Solution processing routes[8–15] were later discovered, which enabled very high-molecular-weight polyethylenes to be processed into high-modulus and high-strength fibres. The best known of these techniques is that of gel-spinning and drawing, which is now used commercially to produce fibres of modulus ~100 GPa and strength ~3 GPa. Much has been written on the mechanisms by which the gel process works (see e.g. refs. 15, 16). Most authors agree that the undrawn gel fibre consists largely of chain-folded, platelet crystals, which themselves deform on the subsequent drawing (to very high draw ratios). The implication is that the undrawn gel fibres are more similar in character to single-crystal mats than to melt-crystallized material, and that it is this special morphology which permits the achievement of high draw ratios. Several authors have worked on the drawing of 'single-crystal mats' of very high-molecular-weight polyethylene, and moduli as high as 220 GPa have been reported[17,18] at draw ratios of ~200. It is interesting to note that the uniqueness of the relationship between modulus and draw ratio initially proposed for melt-crystallized material[4,6,7,19] continues to apply even to these specially prepared materials and at these extremely high draw ratios[16].

Several models (all based on indirect evidence) have been proposed to explain the changes occurring during drawing, to determine the underlying conditions which limit the maximum achievable draw ratios, and to interpret the final mechanical properties in molecular terms[6,15,20–22]. While each of these models can be used to explain some aspect of the drawing behaviour (e.g. modulus, maximum drawability, etc.), none of them can explain all the observed behaviour. We intend in a subsequent paper in this series to discuss models in detail; accordingly, we shall not consider models further here and confine ourselves to the experimental data.

Our concern is to use neutron scattering data to provide firm experimental data on the changes occurring to individual molecules during drawing and, thus, relate directly the molecular extension to the overall extension and the fibre properties. We should note here that a limitation of the neutron scattering techniques is that we cannot look at the behaviour of very large molecules;

0032-3861/90/010046-05$03.00

they give scattering signals at angles that are too low for us to observe. Thus, we cannot obtain any data directly on the fibres of very high modulus and draw ratio described above. In practice we are limited to molecular weights up to ~200 000 and total draw ratios of up to ~40. Nevertheless, we believe that these data can reasonably be extrapolated to the higher molecular weights and draw ratios.

NEUTRON SCATTERING ANALYSIS

We described the methods used to analyse drawn fibres in an earlier publication[23]; we shall simply review the most salient features here. The fibres, which were wound on bobbins, were mounted in the D11 small-angle spectrometer at the Institut Laue–Langevin, Grenoble, with the draw direction horizontal. The beam apertures in the spectrometer are rectangular, with the better collimation in the horizontal direction. The wavelength and specimen-to-detector distances were 8 Å and 9.14 m, and the collimation distances were 10 m (but also, on occasion, 20 and 40 m). The scattering signal from the isotopic blend was considered to be a simple superposition of (i) a signal from the empty apertures, (ii) incoherent scattering, (iii) a coherent scattering signal $I_p(q)$ analogous to that observed in small-angle X-ray scattering, and (iv) the desired molecular scattering $I(q)$ arising from the isotope difference. The quantity q is $4\pi(\sin\theta)/\lambda$, where 2θ is the scattering angle and λ the wavelength. The additivity of $I_p(q)$ and $I(q)$ depends on the corresponding scattering length fluctuations being uncorrelated in space. In practice, simple subtraction procedures also depend on $I_p(q)$ not being large compared with $I(q)$, and being reproducible from one specimen to another. $I_p(q)$ is due to density differences between crystal and disordered regions, cracks (voids) and, possibly, impurities. Drawn samples often fibrillate, which can result in very large intensities $I_p(q)$. This was not the case for the samples used in this study, their appearance being in general translucent. For polyethylene, $I(q)$ can often contain intermolecular as well as intramolecular terms, as a consequence of inhomogeneous isotope distributions[24,25]. These are restricted to very small q values, and are commonly attributed[24] to isotope density fluctuations over large distances as a consequence of fractionation during crystallization.

Figure 1 shows a contour plot of difference intensities for a quenched sheet that has been drawn. The high degree of asymmetry is very striking. The intensity can be expressed as a function of q_x along h (the equator) and q_z along l (the meridian). $I(q_x, 0)$ can readily be obtained by measuring the count rate difference along a line of detector cells parallel to the equator and passing through the beam centre position. The dimension of the molecules along h may be obtained using a Zimm plot, and fitting the data to the equation:

$$I(0,0)/I(q_x,0) = 1 + q_x^2 R_x^2 \qquad (1)$$

where $R_x^2 = \frac{1}{2}(\langle x\rangle^2 + \langle y\rangle^2)$ where x and y are coordinates within the molecule measured from its centre of gravity. Values of $I(0,0)$ and R_x^2 are discussed below.

In order to obtain dimensions along l it is clearly not feasible to take a line of detector cells in a similar way. The region of q from which the dimensions should be obtained are obscured by the backstop region in the centre of *Figure 1*. We have adopted an alternative approach, which not only avoids the problem of missing intensity values near $I(0,0)$ but also makes more efficient use of data than is customary[23].

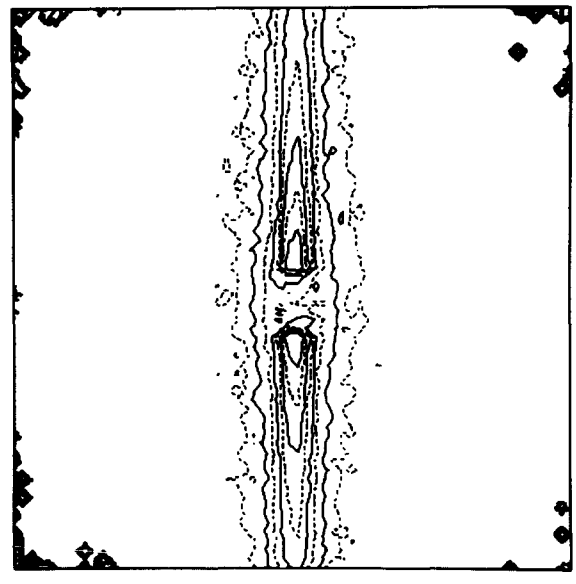

Figure 1 A typical contour plot of the scattered neutron intensity from a highly anisotropic fibre. The fibre direction is horizontal

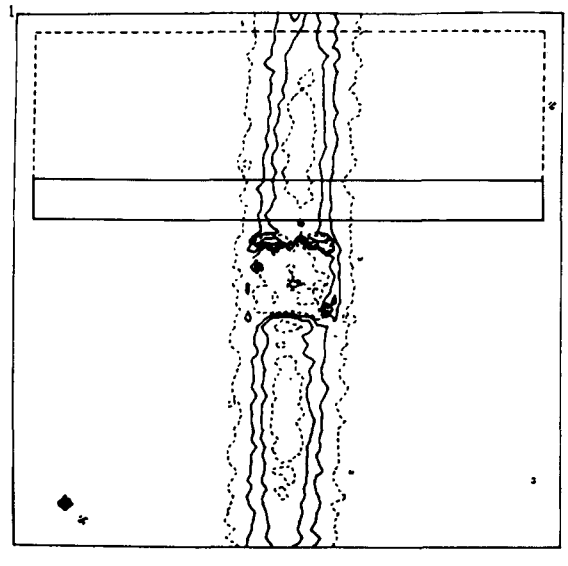

Figure 2 A contour plot from our earlier work[23] showing the rectangles used to calculate R_z values—as described in the text

Intensities were taken from the two-dimensional array by choosing rectangles such as those shown by solid and broken lines in *Figure 2* taken from our earlier work[23]. The intensity *versus* the scattering vector q in the l direction could then be plotted. It was found that the profile of the maximum in such plots was independent of the width of the rectangle for drawn quenched sheets[23].

Information on molecular conformation can be obtained in several ways from intensity as a function of q_z. Molecular dimensions were derived in all cases using the centre part of the peak. About five points can be plotted according to the equation of Zimm for an oriented structure:

$$I(q_x,0)/I(q_x,q_z) = 1 + q_z^2 R_z^2 \qquad (2)$$

where $R_z^2 = \langle z^2\rangle$.

More information can be obtained if the data are fitted

to a model. One possibility is that the projected density corresponds to a 'top hat' function of length d along z. In this case:

$$I(q_x, q_z)/I(q_x, 0) = \sin^2(\tfrac{1}{2}dq_x)/(\tfrac{1}{2}dq_x)^2 \quad (3)$$

On the other hand, several models for the conformation in quenched sheets suggest that, at least on the scale of the whole molecule, the molecular density should be Gaussian. If the molecular deformation were anything approaching affine with the sample deformation, the projected density along z would be the same as the projected density for a Gaussian coil, and:

$$I(q_x, q_z)/I(q_x, 0) = 2/v - (2/v^2)(1 - e^{-v}) \quad (4)$$

where $v = 3R_z^2 q_z^2$. In our earlier paper[23] we showed that the data always gave a better fit to equation (4) than to equation (2). Typically R_z from equation (4) was a little greater than from the Zimm plot of equation (2).

PREPARATION OF THE FIBRES

In all the studies reported here we redrew already necked fibres. The necked fibres used in fact came from those we had previously used to study necking[1,2]. We only used fibres in which there was no evidence for isotopic segregation having occurred during necking. Full details of the changes in molecular dimensions during necking are given in our earlier papers[1,2]. However, we shall briefly summarize the main points here. The three solution-crystallized materials used here all came from the same original mat in which the R_x value was ~ 70 Å and the R_z value (along the chain direction, perpendicular to the draw direction) was ~ 50 Å. After drawing through the neck these values changed so that R_x was ~ 60 Å and R_z (along the chain direction parallel to the draw direction) was ~ 80 Å, the macroscopic draw ratio being ~ 5. The undrawn melt-crystallized material had R_x values of 98 Å (for 64 600 molecular weight) and 170 Å (for 218 000 molecular weight); after necking these decreased, and the actual values are shown in *Table 1*. The molecular draw ratios were, in all cases, similar to the macrosopic draw ratios.

These already necked fibres, whose preparation is described in detail in the previous two papers[1,2], were then drawn further. This was done by stretching the fibres in contact with a heated metal bar at the required drawing temperature. Draw ratios were measured as the ratio of undrawn to drawn mass per unit length. Moduli were measured using an Instron tensile testing machine at an initial strain rate of 10^{-4}; the secant modulus at a strain of 10^{-3} is quoted. In all cases the fibres had aspect ratios exceeding 75, which should be sufficient to avoid errors due to end effects[26].

RESULTS AND DISCUSSION

The results of the neutron scattering experiments are summarized in *Table 1*. We quote first the molecular weights of the dopant deuterated polyethylenes, and the preparation of the initial undrawn samples (either melt-crystallized or single-crystal mats as described in our previous papers[1,2]). Next, we quote data measured on the fibres after necking: the temperature at which drawing through the neck was carried out, the draw ratio across the neck, and the R_x and R_z values derived from Zimm plots as well as the R_z value derived by (trial and error) fitting to equation (4).

We then quote the details of the second drawing: the drawing temperature, the draw ratio (with respect to the already neck-drawn fibre) and the R_x and R_z values from the neutron scattering measurements (we do not consider it reasonable to quote any values for R_z when these are 'measured' to be higher than 1000 Å). We also include the measured values of the modulus of the redrawn fibres. Finally we quote the 'molecular' draw ratios derived from R_x and R_z values. There is a wealth of data in *Table 1*, which we shall discuss and interpret in the following.

First, we note from the last three columns that the molecular draw ratios determined from R_x and two separate R_z estimates are always closely similar; this implies that the molecules deform homogeneously. The values of R_x are inevitably much more accurate than those of R_z, and hence we shall take the molecular draw ratio to be that derived from the R_x values. The second point we wish to note is that we do not observe any sign of isotopic segregation occurring on secondary drawing of already necked fibres, even at secondary drawing temperatures as high as 118°C. This is in marked contrast to the behaviour during necking, where segregation was observed on drawing above 90°C. This observation is, however, not surprising since the secondary drawing occurred homogeneously throughout the samples and was not localized by a neck. Hence, we should not expect any localized melting to occur. It is instructive to examine the relationship between the molecular and fibre draw ratios. A glance at *Table 1* shows that for drawing temperatures of 70 and 77°C the molecular draw ratio is more or less the same as the fibre draw ratio (in all this discussion 'draw ratio' refers to the draw ratio after necking and not to the total fibre draw ratio). At higher drawing temperatures the molecular draw ratio is less than the fibre draw ratio. This is illustrated graphically in *Figure 3*, where we have plotted the molecular draw ratio (from R_x measurements) against the overall draw ratios. The lower molecular draw ratios seen at higher

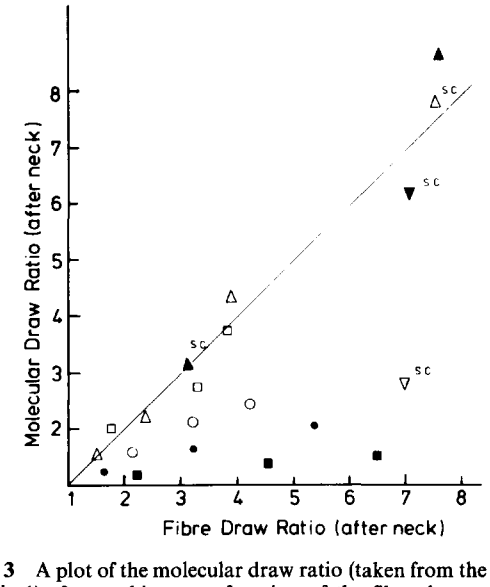

Figure 3 A plot of the molecular draw ratio (taken from the R_x values in *Table 1*) after necking as a function of the fibre draw ratio (after necking). The different symbols refer to the different drawing temperatures. For originally melt-crystallized material: △, 70°C; □, 77°C; ○, 88°C; ●, 98°C; ■, 118°C. For originally solution-crystallized material (marked s.c. on the diagram): ▲, 70°C; ▼, 77°C; ▽, 88°C

Table 1 Results of neutron scattering experiments

DPE mol. wts.			Necking data[a]					Second drawing						Comparisons of molecular draw ratios (after necking)		
M_w	M_n	Method[b]	Temp. (°C)	Draw ratio (macroscopic)	R_x (Å)	R_z (Zimm) (Å)	R_z (eqn (4)) (Å)	Temp. (°C)	Second draw ratio	R_x (Å)	R_z (Zimm) (Å)	R_z (eqn (4)) (Å)	Modulus (GPa)	R_x	R_z (Zimm)	R_z (eqn (4))
64 600	30 500	M	21	8.6	33	430	770	70	1.5	27	620	>1000	8.8	1.5	1.4	>1.3
64 600	30 500	M	42	7.2	36	420	670	70	2.4	24	890	>1000	18	2.2	2.1	>1.5
64 600	30 500	M	42	7.2	36	420	670	70	3.9	17.5	>1000	>1000	84	4.2	>2.4	>1.5
64 600	30 500	SC	78	4.8	64	76	–	70	3.1	35	210	–	22	3.3	2.8	–
64 600	30 500	SC	78	4.8	64	76	–	70	7.5	23	480	–	91	7.8	6.3	–
64 600	30 500	M	21	8.6	33	430	770	77	2.0	25	730	>1000	14	1.7	1.7	>1.3
64 600	30 500	M	69	6.0	43	400	510	77	2.7	24	900	>1000	30	3.2	2.3	>2.0
218 000	69 000	M	72	6.9	65	850	920	77	3.8	34	>1000	>1000	61	3.7	>1.2	>1.1
64 600	30 500	SC	88	5.2	56	86	–	77	7.0	22	510	–	55	6.5	5.9	–
64 600	30 500	M	42	7.2	36	420	670	88	2.1	29	650	950	7.4	1.5	1.5	1.4
64 600	30 500	M	21	8.6	33	430	770	88	3.2	23	850	>1000	19	2.1	2.0	>1.3
64 600	30 500	M	69	6.0	43	400	510	88	4.2	28	900	>1000	22	2.4	2.3	>2.0
64 600	30 500	SC	88	5.2	56	86	–	88	6.9	33	220	–	34	2.9	2.6	–
218 000	69 000	M	20	6.2	76	620	780	98	1.6	69	730	900	5.8	1.2	1.2	1.2
218 000	69 000	M	72	6.9	65	850	920	98	3.2	51	>1000	>1000	11	1.6	>1.2	>1.1
64 600	30 500	M	69	6.8	43	400	510	98	5.4	30	780	>1000	16	2.1	2.0	2.0
64 600	30 500	M	61	7.0	40	400	550	118	2.2	38	430	600	4.8	1.1	1.1	1.1
218 000	69 000	M	54	5.8	72	730	850	118	4.6	61	950	>1000	6.2	1.4	1.3	>1.2
64 600	30 500	M	61	7.0	40	400	550	118	6.5	33	580	820	6.2	1.5	1.5	1.5

[a] Further information about the production of these samples can be found in refs. 1 and 2
[b] M, melt-crystallized; SC, single-crystal mats

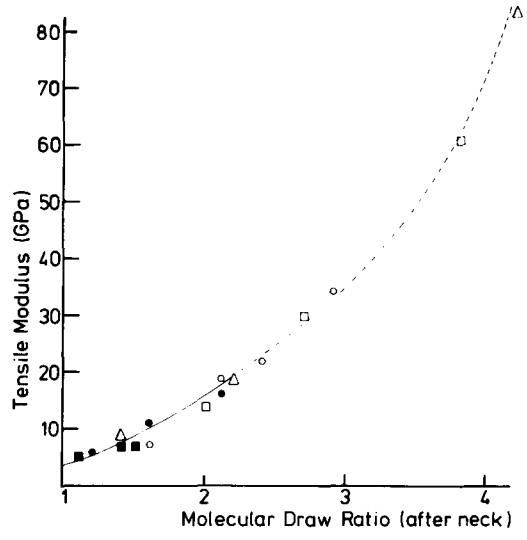

Figure 4 A graph showing the tensile modulus of all the fibres drawn from melt-crystallized material as a function of the molecular draw ratio (from R_x values in *Table 1*). The symbols refer to the different drawing temperatures as in *Figure 3*

drawing temperatures are reflected in the lower values of modulus of these fibres. We suggest that at these higher drawing temperatures there is some viscous flow, which makes the drawing process less effective.

It is well established that the 'effectiveness' of drawing, as assessed by modulus increase, decreases as the drawing temperature increases; however, we can now assess 'effectiveness' in a different way by comparing values of modulus of the fibres drawn from melt-crystallized material with the molecular (rather than the overall) draw ratio. This we have done in *Figure 4*. There is a remarkable correlation suggesting that the final modulus is a unique function of the molecular draw ratio. Thus, the assertion that the modulus is (for 'effective' drawing) a unique function of the fibre draw ratio may be seen to be a consequence of a much more general underlying relationship between the molecular draw ratio and the mechanical properties.

Finally, we wish to make some comments on the apparently affine deformation of individual molecules (at drawing temperatures below ~80°C). We consider, since there is no evidence for melting and recrystallization, and the molecules deform homogeneously and affinely with the whole fibre, that all elements of the fibres also deform affinely. Thus, we suggest that the crystals within the fibres must be extended during fibre drawing, an argument to which we shall return in a future paper concerning models of fibre drawing.

REFERENCES

1 Sadler, D. M. and Barham, P. J. *Polymer* 1990, **31**, 36
2 Sadler, D. M. and Barham, P. J. *Polymer* 1990, **31**, 43
3 Spells, S. J. and Sadler, D. M. *Polymer* 1984, **25**, 739
4 Capaccio, G. and Ward, I. M. *Polymer* 1974, **15**, 233
5 Gibson, A. G., Ward, I. M., Cole, B. N. and Parsons, B. J. *Mater. Sci.* 1974, **9**, 1193
6 Ward, I. M. in 'Ultra-High Modulus Polymers' (Eds. A. Ciferri and I. M. Ward), Applied Science, London, 1982
7 Barham, P. J. and Keller, A. *J. Mater. Sci.* 1976, **11**, 27
8 Zwijnenburg, A. Ph.D. Thesis, Groningen, 1978
9 Zwijnenburg, A. and Pennings, A. J. *Colloid Polym. Sci.* 1978, **259**, 868
10 Smith, P., Lemstra, P. J., Kalb, B. and Pennings, A. J. *Polym. Bull.* 1979, **1**, 733
11 Smith, P. and Lemstra, P. J. *J. Mater. Sci.* 1980, **15**, 505
12 Barham, P. J. and Keller, A. *J. Mater. Sci.* 1980, **15**, 2229
13 Kalb, B. and Pennings, A. J. *J. Mater. Sci.* 1980, **15**, 2584
14 Barham, P. J. *Polymer* 1982, **23**, 1112
15 Smith, P., Lemstra, P. J. and Booij, H. C. *J. Polym. Sci., Polym. Phys. Edn.* 1981, **19**, 877
16 Barham, P. J. and Keller, A. *J. Mater. Sci.* 1985, **20**, 2281
17 Kanamoto, T., Tsurata, A., Tanaka, K., Takeda, M. and Porter, R. S. *Polym. J.* 1983, **15**, 327
18 Furuhata, K., Yokokawa, T. and Miyasaka, K. *J. Polym. Sci., Polym. Phys. Edn.* 1984, **22**, 133
19 Keller, A. in 'Ultra-High Modulus Polymers' (Eds. A. Ciferri and I. M. Ward), Applied Science, London, 1982
20 Barham, P. J. and Arridge, R. G. C. *J. Polym. Sci., Polym. Phys. Edn.* 1977, **15**, 1177
21 Smith, J. B., Davies, G. R., Capaccio, G. and Ward, I. M. *J. Polym. Sci., Polym. Phys. Edn.* 1975, **13**, 2331
22 Peterlin, A. *Colloid Polym. Sci.* 1987, **265**, 357
23 Sadler, D. M. and Barham, P. J. *J. Polym. Sci., Polym. Phys. Edn.* 1983, **21**, 309
24 Sadler, D. M. and Keller, A. *Macromolecules* 1977, **10**, 1128
25 Schelten, J., Ballard, D. G. H., Wignall, G. D., Longman, C. and Schmatz, W. *Polymer* 1976, **17**, 751
26 Arridge, R. G. C., Barham, P. J., Farrell, C. J. and Keller, A. *J. Mater. Sci.* 1976, **11**, 788